International Journal of Modern Physics C
Vol. 20, No. 7 (2009) 1049–1062

World Scientific
www.worldscientific.com

EFFECT OF MEMORY AND REINFORCEMENT ON THE PROPAGATION AND MORPHOLOGY OF FRACTURE IN A TWO-DIMENSIONAL MASS-SPRING SYSTEM

GEORGE ALLAN ESLETA and CHRISTOPHER MONTEROLA*
National Institute of Physics, University of the Philippines
Diliman Quezon City 1101, Philippines
**cmonterola@gmail.com*

Received 16 February 2009
Accepted 21 March 2009

We investigate the interplay of damage accumulation and structural reinforcement in the fatigue failure of a two-dimensional mass-spring system. Damage accumulation is captured in the model such that the damage of a spring at a certain time depends on its entire deformation history. Structural reinforcement, on the other hand, is implemented by increasing the breaking thresholds of the springs [Esleta and Monterola, *Comp. Phys. Comm.* 2008[1]]. We demonstrate that consistent with known empirical laws, in the presence of memory, the lifetime t_f of the system subjected to a stress amplitude σ_0 is a power law ($t_f \sim \sigma_0^{-\gamma}$). As damage accumulation memory f_0 is incorporated into the system, the transition from non-power law ($f_0 = 0$, no memory) to power law distribution is observed. Preservation of the power law behavior (equal value of γ) is guaranteed even when the system's lifetime is prolonged through static reinforcement. Finally, our model demonstrates that strengthening the stress memory of spring elements leads to more scattered crack patterns, a result that agrees phenomenologically with existing experiments.

Keywords: Fracture; fatigue; damage accumulation; memory; reinforcement.

PACS Nos.: 11.25.Hf, 123.1K.

1. Introduction

Fracture, or the break-up of a material under the action of stress, is universal in a sense that it occurs under a variety of conditions and in many types of materials. It is observed on a broad range of length scales, from the fragmentation of molecules, the cracking of asphalt roads, up to geological phenomena such as earthquakes.[2–4] This process usually starts with the formation of cracks in the microscopic level. As stress is continuously applied to the specimen, these cracks may grow and propagate, leading to structural failure. A detailed understanding of the mechanisms

behind crack formation and propagation is important in improving the reliability of structures, and preventing unwanted damage to life and property.

The ability of a material to resist fracture is dependent on its tensile strength. Both experiments and numerical studies have shown that macroscopic failure occurs instantaneously when a material is subjected to a force above its tensile strength limit.[5] For stresses below this limit, failure may still occur but only after repeated application of the stress. This fatigue process, or the progressive deterioration of a material under subcritical loading, accounts for most failures in cyclic devices such as engines.

Structural engineers determine the fatigue strength of a material by applying different load strengths to individual specimens and measuring the *lifetime* or the number of cycles before failure occurs. Fatigue life is usually large and in the order of $\sim 10^3$ cycles, but this decreases as the load amplitude is increased. In 1910, O. H. Basquin noted that the decrease in lifetime of most materials is a power law of increasing stress amplitude σ_0, or $t_f \sim \sigma_0^{-\gamma}$.[6] The fundamental principle on the emergence of Basquin's law in materials undergoing fatigue failure is a subject of intense research among engineers, physicists and material scientists. Recently, using a fiber bundle model (FBM) and a discrete element model (DEM), it was shown that this scaling law is a direct consequence of damage accumulation in the microscopic scale.[7]

Most of the existing knowledge about fatigue failure relies on experimental observations. Material modeling is becoming an important tool for improving structural design and preventing the onset of fatigue. One possible way to change the durability of a material is by introducing randomness or disorder. It has been known that inhomogeneities in a material has profound effects on its strength, since fracture typically starts from weaker spots such as preexisting cracks or voids.[8] By changing the distribution of failure thresholds in the material, it is possible to improve its resistance to fracture, delay the onset of tearing and minimize tear propagation.[1]

In this paper we extend our 2D mass-spring model of fracture propagation[1] by incorporating stress memory to the spring elements. In the model, the material is composed of a large number of point particles that are coupled by breakable springs. We derive the full nonlinear equations for the forces in terms of displacements, and use them to follow the time evolution of the system as it undergoes uniaxial stretching. Similar to the work of Kun *et al.*,[7,9] an ageing mechanism is introduced, i.e. all intact springs undergo a damage accumulation process which can again give rise to breaking. We study in detail the time evolution of a rectangular sample under uniaxial stretching and show that the addition of memory causes the material to obey Basquin's law of fatigue ($t_f \sim \sigma_0^{-\gamma}$). Increasing the strength of the memory also causes the fractures to be more scattered. Lastly, we look into the robustness of the characteristic exponent γ by varying the distribution of failure thresholds.

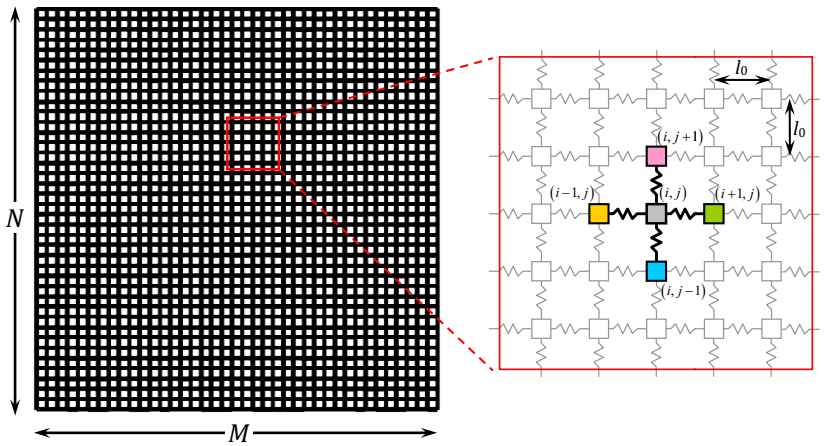

Fig. 1. Model architecture and index conventions. The lattice sites represent point-like material elements with identical masses m. Neighboring masses are connected by linear elastic springs with unstretched lengths l_0 and stiffness κ. Free boundary conditions (FBC) are used, with three neighbors at the edges and two at corners.

2. Two-Dimensional Mass-Spring Model

Our model system is shown in Fig. 1: a regular M by N square lattice with lattice spacing l_0. We have previously used this system to characterize the fragmentation and structural reinforcement of elastic materials.[1] The material is assumed to be composed of a large number of identical particles that interact elastically with each other.

The lattice sites, labeled by (i, j) where $1 \leq i \leq M$ and $1 \leq j \leq N$, contain identical point particles with mass m. For simplicity and ease of computation, the motion of the (i, j)th mass is constrained to two dimensions $x_{i,j}$ and $y_{i,j}$, such that the displacement vector of node (i, j) is $\mathbf{r}_{i,j} \equiv x_{i,j}\hat{i} + y_{i,j}\hat{j}$.

The elastic behavior of solids is captured in the model by the inclusion of identical springs with stiffness κ and unstretched length l_0 between neighboring particles. Simple Hookean springs are used, so that the force exerted by a spring is just proportional to its elongation $\Delta l \equiv l - l_0$, with κ being the constant of proportionality. The connections are then made following the Von Neumann neighborhood, wherein a lattice site is connected to its four nearest neighbors at the top, bottom, left and right. As shown in Fig. 1, the particle in location (i, j) is connected to the particles at positions $(i-1, j)$, $(i+1, j)$, $(i, j-1)$ and $(i, j+1)$.

Following the work of Olami,[10,11] free boundary conditions are also imposed in our lattice model. As a result, points at the lattice edges [i.e. $(1, j)$, (M, j), $(i, 1)$, and (i, N), where $1 < i < M$ and $1 < j < N$] have three neighbors each. Points at the lattice corners, i.e. $(1, 1)$, $(1, N)$, $(M, 1)$, and (M, N), on the other hand, have only two neighbors.

To incorporate tear propagation in the model, a simple tearing mechanism is implemented as outlined in Fig. 2. Initially, each spring is assigned a unique elongation threshold ε_{th} which controls when the spring will break. In the course of the simulation, a spring will break when its deformation $\Delta l \equiv l - l_0$ reaches or

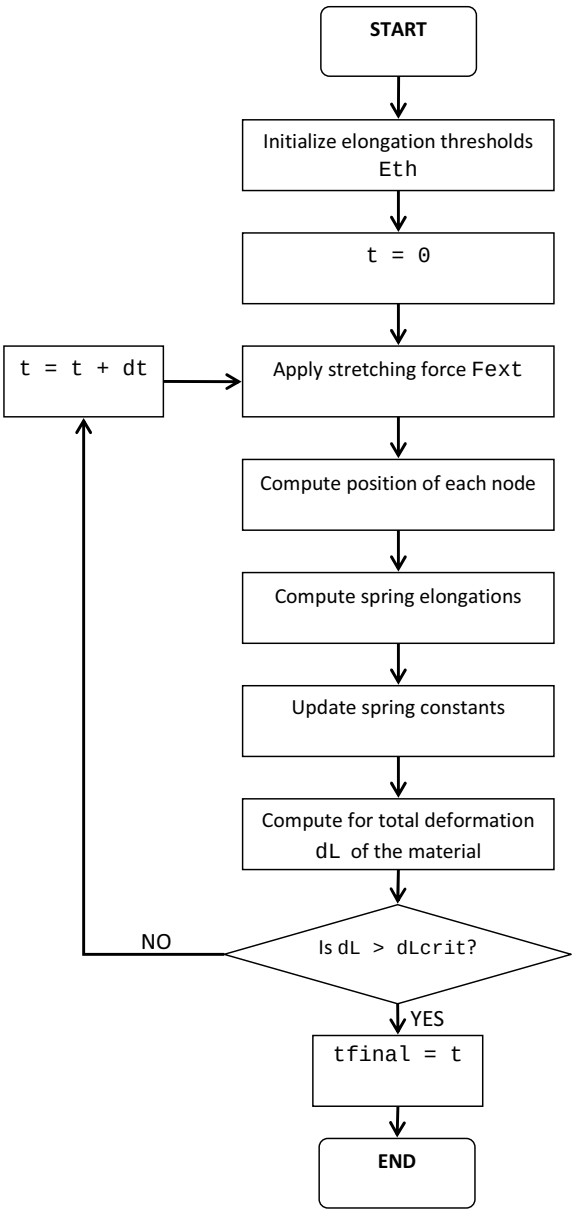

Fig. 2. Flowchart of the simulation algorithm.

exceeds the designated elongation threshold. Once a spring breaks, it releases its stored energy and redistributes it to neighboring springs. As a result, there will be a cascade of spring failure, which will eventually cause macroscopic failure.

Previously we show that a material may be engineered so as to prevent fatigue failure and prolong lifetime, and one way to do this is by varying the distribution of elongation thresholds in the lattice.[1] The elongation thresholds may be assigned either randomly or by following a certain spatial distribution (e.g. Gaussian). The various procedures for assigning the elongation thresholds will be discussed in a later section.

After assigning the elongation threshold of the springs, the time evolution of the lattice is followed by solving the equations of motion of the individual particles using an iterative fourth order Runge–Kutta method. For each time step, external load is imposed on the lattice by adding a constant outward force $F_{\text{ext}}(t) \equiv F_{\text{ext}}$ at the left and right edges:

$$\mathbf{f}_L = \begin{cases} -F_{\text{ext}}\hat{i}\,, & i = 1 \qquad \text{(left edge)} \\ F_{\text{ext}}\hat{i}\,, & i = L \qquad \text{(right edge)} \\ 0\,, & \text{elsewhere} \end{cases} \tag{1}$$

In effect, the material is stretched horizontally with a constant external force F_{ext}. The uniaxial stretching is analogous to the experimental procedure implemented by Kim and Shim to analyze the scattering of the fatigue crack growth of aluminum sheet.[12] After solving for the displacement of each particle in the lattice, the condition for breaking is evaluated for all intact springs. The elongation of the springs are computed, and if the elongation of a spring exceeds ε, its stiffness is assigned a zero value and is removed from further calculations. The breaking of springs is irreversible, which means that it is excluded from the force calculations in the proceeding timesteps. The simulation will continue until the total deformation of the system exceeds a critical value.

3. Damage Accumulation

An important characteristic of the fatigue process is that it is cumulative and irreversible. Once crack formation starts, it is not possible for the material to recover or heal. Instead, more damage appears in the microscopic level and the cracks grow. The accumulation of cracks and other kinds of microscopic damage will eventually cause the material to disintegrate even if the instantaneous stress is below the tensile limit. We investigate in the next subsections the lifetime and morphology of propagating cracks in our system as the strength of damage accumulation memory is increased.

3.1. *Implementation*

To model the process of damage accumulation in the material, we modified the tearing dynamics and implemented a new spring breaking rule similar to that of

Carmona *et al.*[13] Each spring has a *memory* of its deformation history, which can be visualized as a sequence of numbers $\{\varepsilon(0), \varepsilon(\delta t), \varepsilon(2\delta t), \ldots, \varepsilon(t)\}$. The first number in the sequence corresponds to the spring's deformation at $t = 0$, and the succeeding numbers correspond to the deformation at each timestep. At the start of the simulation, the spring's memory contains no information. After one iteration, the deformation of the spring is computed and it is appended at the end of the "sequence." The process is repeated for the succeeding timesteps. As a result, the memory grows linearly in time. For simplicity, the memory of the springs are long-term, i.e. the spring stores its *entire* deformation history completely and does not truncate it. In Carmona's model this is equivalent to having an infinite memory range.

The accumulated damage q_a of a spring at a certain time t is then obtained by summing over the spring's entire history:

$$q_a(t) = f_0 \sum_{t'=0}^{t'=t} \varepsilon(t') \tag{2}$$

where f_0 is a scaling parameter that controls the strength of memory. To determine if spring breaking will take place, we evaluate the *total damage* $q(t)$ of a spring, which takes into account the instantaneous deformation $\varepsilon(t)$ and the accumulated damage $q_a(t)$:

$$q(t) = \varepsilon(t) + f_0 \sum_{t'=0}^{t'=t} \varepsilon(t')\,. \tag{3}$$

A spring then breaks when its total damage exceeds the elongation threshold ε_{th}. This is essentially a modification of Kun's model where the healing factor is removed.[13] The first term in Eq. (3) accounts for spring damage due to *immediate breaking*, while the second term accounts for *damage accumulation* as a result of continuous loading. The relative importance of these two damage mechanisms is controlled by the memory factor f_0. When f_0 is significantly large, damage accumulation dominates. For each timestep, the total damage of all springs are evaluated, and those springs for which $q(t) > \varepsilon_{th}$ are considered to be broken, i.e. are removed from the simulation. Note that if $f_0 = 0$ we simply go back to the original breaking rule.

Simulations were performed over a wide range of values of the memory factor and the applied force, using a lattice size $L = 40$. Table 1 summarizes the parameter values used in the simulations. Without loss of generality, we choose our units such that $l_0 = 1$, $m = 1$, and $\kappa = 1$.[1] To introduce disorder in the material, the springs were assigned elongation threshold values randomly chosen within the range $[\varepsilon_{th}, 1.10\varepsilon_{th}]$. At the start of the simulation the nodes are at rest and at their initial positions. The specimen is then loaded by applying a constant force F at the left and right edges, and its time evolution is followed by solving the equations of motion using a fourth order Runge–Kutta method with timestep $\delta t = 2^{-4}$. The

Table 1. Parameter values used in the simulation.

Parameter		Value
Lattice size	N	40
Timestep	δt	2^{-4}
Memory factor	f_0	$0.005 - 0.5$
Elongation threshold	ε_{th}	0.05

breaking rule is evaluated at each timestep for all the intact springs. When a spring's deformation exceeds the elongation threshold, its stiffness is assigned a zero value and is excluded from the force calculations in the proceeding timesteps. The above simulation parameters are shown to capture the behavior of larger lattice, with the advantage of lesser computational complexity.[1]

3.2. *Morphology of crack patterns and lifetime of model systems*

We apply our model to simulate the fatigue failure of a rectangular sample under time-invariant, unidirectional stress. The 40×40 rectangular lattice is subjected to a constant force F on opposite ends that is slowly increased from zero to avoid the buildup of elastic waves.[13] During this process of gradual loading, the springs remain intact and the conditions for breaking are not applied. Only when the applied force reaches the value F are the breaking rules implemented. We define the lifetime t_f of the material to be the time when the system reaches its maximum unidirectional deformation given by $(N-1) * \varepsilon_{th}$.

To understand how the introduction of damage accumulation influence the fracture process, we first look at the time evolution of the system for different values of the memory factor f_0. Shown in Fig. 3 are snapshots of the fatigue process for a specimen with memory factor $f_0 = 0.01$ stretched with a force $F = 0.008$. The specimen remains intact for quite some time, and only at around $t = 1880$ did cracks start to appear. The first micro-cracks are formed at the center of the sample, then grew and propagated in a direction perpendicular to the applied stress. Crack propagation is rapid, and it only took around $\sim$160 time units for the material to completely break-up. This agrees well with previous experimental observations on the fatigue process: a long waiting time and then a rapid failure.[9] Such time-scale separation of low and fast processes is a known signature of self-organized critical

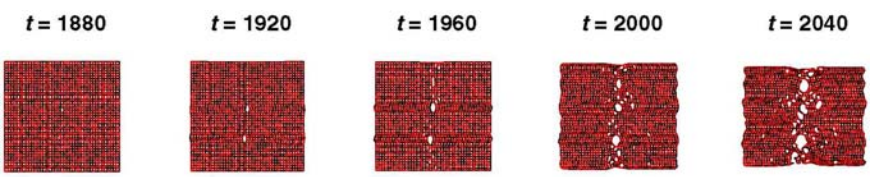

Fig. 3. Time evolution of a 40×40 lattice with memory factor $f_0 = 0.01$. Material remains intact from $t = 0$ to about $t = 1880$.

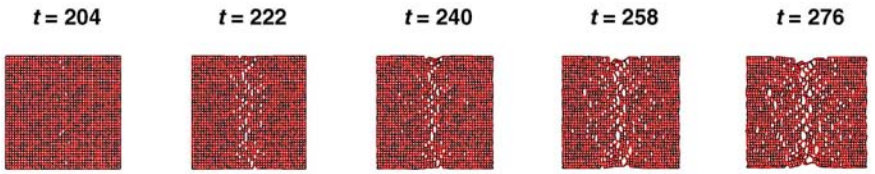

Fig. 4. Time evolution of a 40×40 lattice with memory factor $f_0 = 0.10$. Material remains intact from $t = 0$ to about $t = 204$.

systems, and is achieved in our model system by inducing stress buildup through memory of deformation history.[14,15]

Increasing the memory of the material has a profound effect on the fatigue life and the resulting crack morphology. Shown in Fig. 4 is the time evolution of a specimen with a higher memory factor $f_0 = 0.10$ stretched with the same force ($F = 0.008$). For this sample a significantly shorter waiting time (from $t = 1880$ to $t = 204$) is needed for the first micro-cracks to appear. An increase in memory clearly reduces a material's lifetime. Crack propagation is still in a direction normal to the applied force, and fatigue failure occurred $\sim$72 time units after the first cracks appeared. There is a notable difference, however, on the spatial distribution of the cracks. A larger memory seems to cause the cracks to be more scattered throughout the sample.

Figure 5 compares the final crack patterns for different values of f_0, with the applied force kept constant. When damage accumulation is almost negligible, as in the case of $f_0 = 0.01$, the cracks are observed to be constrained in the center of

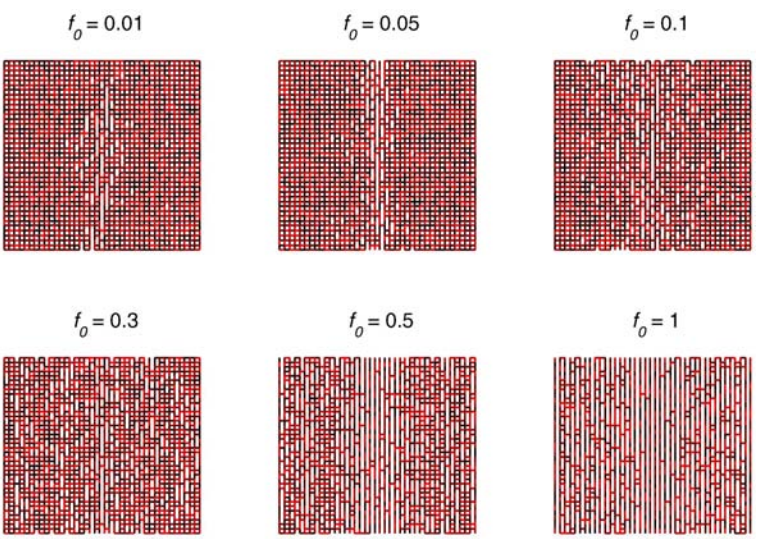

Fig. 5. Final fracture pattern for different memory factor f_0. The 40×40 lattice is stretched using a horizontal force of $F = 0.008$.

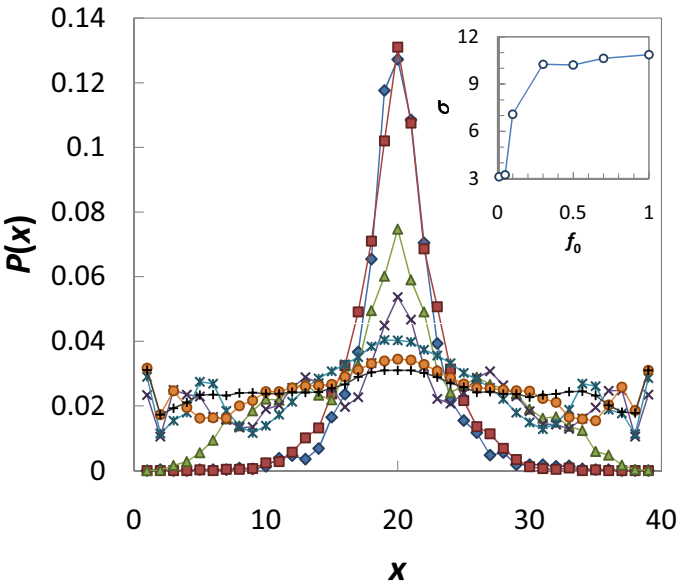

Fig. 6. (Color online) Normalized spatial crack distribution corresponding to the crack patterns shown in Fig. 5 for: $f_0 = 0.01$ (red square), $f_0 = 0.05$ (blue diamond), $f_0 = 0.10$ (green triangle), $f_0 = 0.30$ (violet x), $f_0 = 0.50$ (blue $*$), $f_0 = 0.70$ (orange circle), $f_0 = 1.0$ (black $+$). The 40×40 lattice is stretched using a horizontal force of $F = 0.008$. Inset: The standard deviation σ of the spatial crack distribution for different f_0.

the specimen. This suggests that for low enough f_0, failure process is dominated by stress enhancement in the vicinity of existing cracks favoring localized crack growth. On the other hand, for high enough f_0, the damage propagation becomes more disorder-driven so that cracks are spread all over the system. The degree of dispersion can extend up to a point wherein the cracks become distributed throughout the entire sample, as shown in Fig. 5.

We quantify the crack dispersion by plotting in Fig. 6 the normalized distribution of cracks in the sample. For all values of f_0 the crack distribution has a peak in the center of the sample. As f_0 increases, the height of the peak decreases while the variance σ of the distribution increases (see inset of Fig. 6), indicating crack dispersion. From the inset of Fig. 6 we see that from $\sigma \sim 3$ for $f_0 \leq 0.05$, the variance approaches asymptotically $\sigma \sim 11$ for $f_0 > 0.30$.

Our numerical experiments suggest that increasing f_0 will increase the local stress close to the horizontal free ends ($x = 1$ and $x = 40$ in Fig. 6). This is expected since the free ends is the first to experience the external force F, and hence the larger is the memory f_0, the faster the springs near the applied F approach the tensile limit. For sufficiently large f_0 ($f_0 > 0.1$), this translates to the possibility of broken springs (or "seed cracks") not originating from the center. The off-center cracks are then viewed as a result of the balance between:

(i) the propagating high local stress applied at the free ends, and
(ii) decay of propagating local stress from the center.

Since "seed cracks" favor localized crack growth as previously discussed, the system will eventually have peaks different from the middle peak. The wavelike spreading of the resulting crack distribution (see Fig. 6) as f_0 is varied is indicative of interfering elastic waves during the application of F.

The above results phenomenologically capture the features of the experiments and statistical model of Kim and Shim[12] showing that fatigue crack growth of thinner specimens produces larger scattering of cracks. In their setup, they look at the crack morphology of aluminum alloy subjected to a single tensile overload, corresponding to the uniaxial stretching in our simulation. We conjecture that the correlation of increasing thickness is decreasing the strength of the memory factor f_0. Such relation is intuitive since the effective damage of a single stress cycle is smaller for thicker specimen (or damage is larger per stress cycle for thinner specimen).

From the snapshots of the fracture process shown in Figs. 3 and 4, it is evident that an increase in the memory factor f_0 shortens the lifetime of the specimen. Again, by phenomenologically noting that thickness is the inverse of f_0, we satisfy an intuitive relation that decreasing the thickness (increase of f_0) shortens the lifetime of a stretched material.[12]

We now perform simulations to determine the statistical dependence of the sample's lifetime on the magnitude of the applied stress. Figure 7 presents the variation of the lifetime t_f with the external force F for different values of f_0. For all curves the lifetime decreases rapidly with increasing F. The lifetime exhibits a power law behavior $t_f \sim F^{-\gamma}$ for forces less than $\sim$0.01, which is in agreement with previous experimental and theoretical observations.[6,7,13] The value of the Basquin exponent γ is dependent on f_0, varying from $\gamma \cong -2.1$ for $f_0 = 0.005$ ($R^2 = 0.94$) to $\gamma \cong -1.8$ for $f_0 = 0.05$ ($R^2 = 0.99$).

Note that there is a significant deviation from the power law behavior when F is greater than F_{limit} (~ 0.018) — the point when the applied force exceeds the material's tensile strength. In this region, the lifetime drops rapidly and fatigue failure is almost instantaneous. When the stress memory is absent ($f_0 = 0$) *and* the applied force is less than the tensile limit ($F < F_{\text{limit}} \sim 0.018$), the system's lifetime approaches infinity as expected (see Fig. 7).

4. Structural Reinforcement

4.1. *Implementation*

We hinder the process of damage accumulation by reinforcing the thresholds of the spring using the reinforcement parameter α, which is related to the ratio of elongation thresholds before and after reinforcement. If ε_{th} and ε'_{th} are the elongation

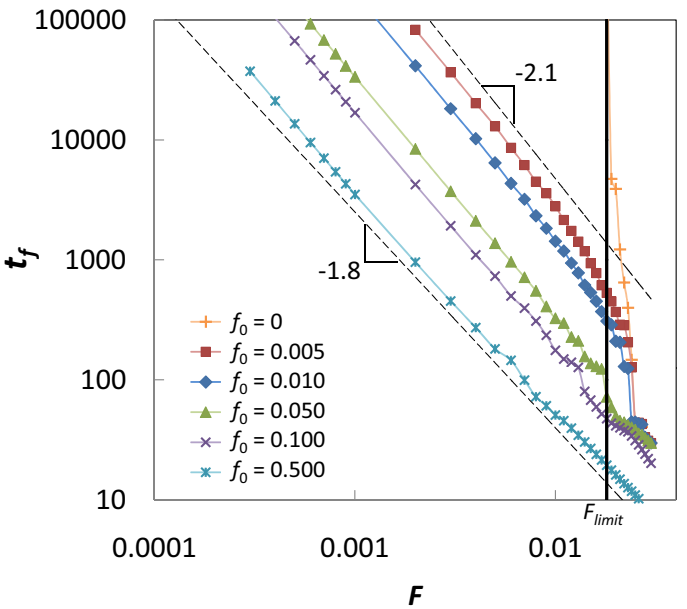

Fig. 7. Lifetime t_f of the mass spring system as a function of applied force F for different values of the memory factor f_0. For $f_0 \geq 0.005$, the lifetime is a power law for applied forces F below the tensile limit F_{limit} (solid vertical line). For $f_0 = 0$, the lifetime is not a power law and is characterized by: (1) t_F approaching infinity for $F < F_{\text{limit}}$ ($= 0.018$), and (2) t_F decaying very fast for $F > F_{\text{limit}}$ ($\sim \exp^{-808F}$, $R^2 = 0.85$).

thresholds of a spring before and after reinforcement, respectively, then

$$\alpha = \frac{\sum \varepsilon'_{th}}{\sum \varepsilon_{th}} - 1 \tag{4}$$

where the summation is done for all springs in the lattice. A zero value of α means that the material is unreinforced.

Aside from increasing the elastic thresholds, it is also important how the reinforcements are distributed throughout the material. In the simulations three static spatial distributions have been considered: (i) *random*, (ii) *Gaussian*, and (iii) *inverted Gaussian*. The above configurations are chosen because of their previous success in increasing the lifetime and delaying the onset of tearing of the two-dimensional mass-spring system.[1] Figure 8 provides a visual representation of each distribution. The values of the failure threshold varies from black (lowest) to red (intermediate) to yellow (highest). In the random case shown on Fig. 8(a), the reinforcements are placed randomly through the lattice. If $\varepsilon_{th}^{(i,j)}$ is the elastic threshold of the spring at node (i, j), its new value after reinforcement is

$$\varepsilon_{th}^{(i,j)'} \sim \varepsilon_{th}^{(i,j)} + A\zeta \tag{5}$$

where ζ is a random number between 0 and 1, and A is a normalization constant that depends on the value of the reinforcement parameter α. For the Gaussian case

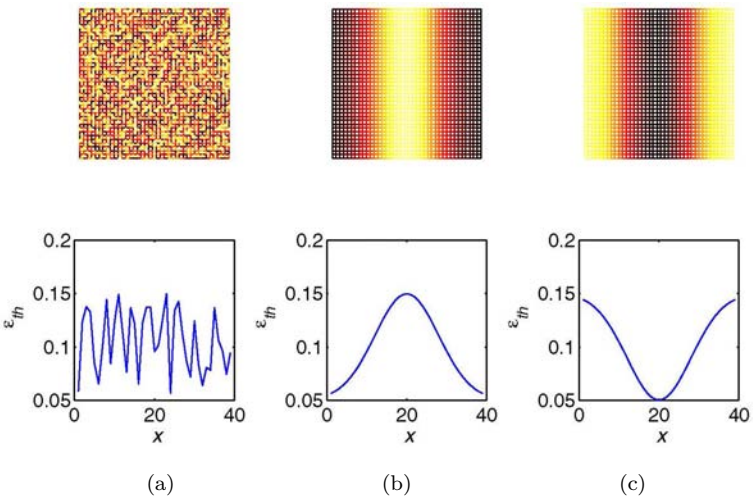

Fig. 8. (Color online) Resulting failure threshold distributions for (a) random; (b) Gaussian; (c) inverted Gaussian. The values of the failure threshold varies from black (lowest) to red (intermediate) to yellow (highest).

shown on Fig. 8(b) the elastic thresholds are updated according to

$$\varepsilon_{th}^{(i,j)'} \sim \varepsilon_{th}^{(i,j)} + A \exp\left\{-\frac{[i-0.5(N+1)]^2}{2\sigma^2}\right\} \tag{6}$$

where σ is the spread of the distribution. Lastly, for the inverse Gaussian case shown on Fig. 8(c), the thresholds follow the distribution

$$\varepsilon_{th}^{(i,j)'} \sim \varepsilon_{th}^{(i,j)} + A\left(1 - \exp\left\{-\frac{[i-0.5(N+1)]^2}{2\sigma^2}\right\}\right) . \tag{7}$$

In all cases the reinforcements are normalized depending on the value of the reinforcement parameter α.

For all reinforcement procedures, simulations were performed using a lattice size $L = 40$ over a wide range of values of the parameters F_{ext} and α. Prior to reinforcement, all springs have identical failure thresholds $\varepsilon_{th} \equiv 0.05$. After increasing the values of the failure thresholds based on the chosen reinforcement strategy, the lattice is stretched with an external force given by Eq. (1). The time evolution of the system is followed by solving the equations of motion with the condition for breaking evaluated for all the intact springs at each iteration.

4.2. *Robustness of Basquin's law*

We investigate the effect of structural reinforcement on the robustness of the observed power law behavior of lifetime or Basquin's law. Numerical experiments are performed by varying the amount of reinforcement α and the reinforcement procedure. Figure 9(a) shows the dependence of the lifetime on the applied force for

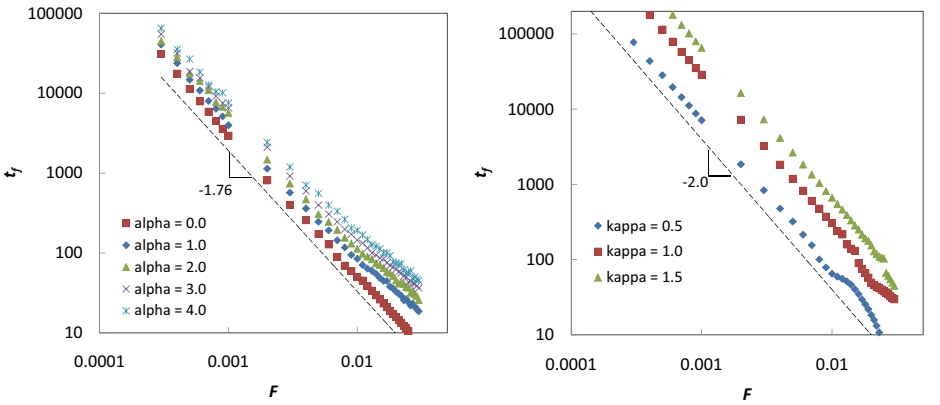

Fig. 9. (Color online) Lifetime as a function of applied force for different values of the (a) reinforcement parameter α, and (b) stiffness κ.

different values of α using a random distribution of reinforcements. In all cases a specimen with a high memory factor $f_0 = 0.5$ is used. The same power law behavior $t_f \sim F^{-\gamma}$ is exhibited by the curves for forces less than $\sim$0.01. We have observed that the value of α has statistically negligible effect on Basquin's exponent ($\gamma \approx -1.76$) of the mass-spring system. Hence, it is apparent that the value of γ depends solely on the amount of memory. However, α causes the t_f vs F graph to shift upward implying a power law distributed increase in the lifetime of the system.

The sample is also reinforced by increasing the stiffness κ of the springs. Figure 9(b) shows the t_f vs F for different values of κ. Increasing the value of κ only shifts the graph upwards, indicating prolonged lifetime. The value of the exponent however is invariant with κ. The results suggest that Basquin's law induced by damage accumulation process in a mass-spring model, is invariant to reinforcement and material disorder. Structural reinforcement, whether by increasing ε_{th} or by increasing κ, only shifts the t_f vs F curve upward, prolonging the lifetime of the sample. We note the similarity of this behavior to the sandpile model[16] where the threshold value will not affect the power law exponent (equal to -1) of the avalanche size distribution. Here, the cascading nature of fracture propagation is the analog of the cascade of avalanches in the sandpile model.

5. Conclusions

We have incorporated the effects of damage accumulation in the fracture propagation of a two-dimensional mass-spring system. In the model, the material is composed of a large number of point particles that are coupled by breakable springs. Numerical simulations are performed to study the time evolution of a rectangular specimen under uniaxial stretching, using different values of memory factor f_0. We

have observed that the morphology of crack patterns can be parametrized by f_0 such that it becomes more scattered as f_0 is increased. More importantly, the model system obeys Basquin's Law of Fatigue, with the exponent showing invariance to structural reinforcement and material disorder.

References

1. G. A. Esleta and C. Monterola, *Comput. Phys. Commun.* **178**, 9 (2008).
2. R. Burridge and L. Knopoff, *Bulletin of the Seismological Society of America* **57**, 341 (1967).
3. K. Chen, P. Bak and S. P. Obukhov, *Phys. Rev. A* **43**, 2 (1991).
4. K. Leung, J. Müller and J. V. Andersen, *J. de Phys. I* **7**, 423 (1997).
5. F. Kun, M. H. Costa, R. N. Costa Filho, J. S. Andrade, Jr., J. B. Soares, S. Zapperi and H. J. Herrmann, *J. Stat. Mech.* p02003 (2007).
6. O. H. Basquin, *Proc. American Society of Testing Materials ASTEA* **10**, 625 (1910).
7. F. Kun, H. A. Carmona, J. S. Andrade, Jr. and H. J. Herrmann, *Phys. Rev. Lett.* **100**, 094301 (2008).
8. M. Alava, P. K. Nukala and S. Zapperi, *Adv. Phys.* **55**, 349 (2006).
9. F. Kun, Z. Halasz, J. S. Andrade, Jr. and H. J. Herrmann, *J. Stat. Mech.* P01021 (2009).
10. Z. Olami, J. S. Feder and K. Christensen, *Phys. Rev. Lett.* **68**, 1244 (1992).
11. K. Christensen and Z. Olami, *Phys. Rev. A* **45**, 665 (1992).
12. J. Kim and D. Shim, *Int. J. Fatigue* **25**, 611 (2003).
13. H. A. Carmona, F. Kun, J. S. Andrade, Jr. and H. J. Herrmann, *Phys. Rev. E* **75**, 046115 (2007).
14. D. E. Juanico, A. Longjas, R. Batac and C. Monterola, *Geophys. Rev. Lett.* **35**, L19403 (2008).
15. D. E. Juanico and C. Monterola, *J. Phys. A* **40**, 9297 (2007).
16. P. Bak, *How Nature Works: The Science of Self-Organized Criticality* (Copernicus, 1996).